Magnetic moment of Fe_3O_4 films with thicknesses near the unit-cell size

G. F. M. Gomes,[1,*] T. E. P. Bueno,[1] D. E. Parreiras,[1] G. J. P. Abreu,[2] A. de Siervo,[2] J. C. Cezar,[3] H.-D. Pfannes,[1] and R. Paniago[1]

[1]*Departamento de Física, ICEx, Universidade Federal de Minas Gerais, 31270-901 Belo Horizonte, MG, Brazil*

[2]*Instituto de Física Gleb Wataghin, Universidade Estadual de Campinas, 13083-859 Campinas, SP, Brazil*

[3]*Laboratório Nacional de Luz Síncrotron, C.P. 6192, 13083-970 Campinas, SP, Brazil*

(Received 9 July 2014; revised manuscript received 2 October 2014; published 28 October 2014)

We perform a systematic study on the evolution of the magnetic spin moment (m_s) of epitaxial [100]- and [111]-magnetite films of increasing thickness. The ultrathin films are characterized by low-energy electron diffraction, x-ray absorption spectroscopy, and x-ray magnetic circular dichroism (XMCD). By employing sum rules on the XMCD spectra we obtain $m_s = 3.6\ \mu_B$/f.u. for samples of around 35 Å. This is considered a bulk value and has been reported only for films more than 10 times thicker. Moreover, we show that even 10-Å-thick magnetite already presents a significant magnetic moment. For both grown directions the moment increases similarly with the thickness. The ferromagnetic behavior for each iron ion site (Fe^{2+}_{octa}, Fe^{3+}_{octa}, Fe^{3+}_{tetra}) of Fe_3O_4 is measured by monitoring XMCD peaks. The deduced hysteresis curves (per ion, per site) exhibit a coercive field of 300 Oe. Our results show that both the ferrimagnetic order and the bulk moment value are preserved at room temperature around the thickness of 2 unit cells.

DOI: 10.1103/PhysRevB.90.134422 PACS number(s): 75.70.Ak, 78.20.Ls, 75.47.Lx

I. INTRODUCTION

Magnetite has attracted much interest due to the applicability of its unique properties, such as half-metallicity, a high Curie temperature, and large spin polarization. However, the magnetic properties of ultrathin Fe_3O_4 can differ from those of the bulk, e.g., the Verwey temperature and the magnetic spin moment decrease [1–5], and superparamagnetism arises [6–8]. Despite the great interest in magnetite there are only few studies dealing with the magnetic behavior of films less than 50 Å thick [1–4,6–13]. Furthermore, it is difficult to obtain Fe_3O_4 films composed of a few monolayers without the formation of islands, oxygen, or iron vacancies and the formation of antiphase boundaries [7,8,11]. These nondesired effects can significantly change the magnetic response. An important question is how the magnetic moment of Fe_3O_4 behaves near the unit-cell limit. While some authors report stable ferrimagnetism for films of around 30 Å [1,2,4,9,12,13], others observe superparamagnetism [6–8]. X-Ray magnetic circular dichroism (XMCD)—the difference between the x-ray absorption spectroscopies (XASs) of two opposite light helicities—is one of the most powerful techniques for investigation of the magnetic behavior of nanoscale structures with element specificity. XMCD at the $L_{2,3}$ edge of transition elements is now widely used as a local probe for the site symmetry [14]. Moreover, the spin (m_s) and orbital (m_l) moments can be calculated using sum rules [15].

The magnetic spin moments for ultrathin magnetite as determined experimentally by various groups present much lower values than the bulk spin moment, which is very intriguing. Another open question is what is the lowest thickness required to maintain the bulk ferrimagnetic order at room temperature. Using XMCD, Monti *et al.* [9] have shown that even 2-unit-cell-thick Fe_3O_4(111) can have the ferrimagnetic order preserved up to 520 K. Babu *et al.* [2] have investigated Fe_3O_4 (12–25 Å) on $BaTiO_3$(100) by XMCD and observed an increase in both the dichroic signal and the magnetic spin moment with increasing film thickness. For the thicker film they found $m_s = 1.45\mu_B$/f.u. (per formula unit), far from the theoretical value ($4\mu_B$/f.u.), and argued that a γ-Fe_2O_3 phase may have been formed, contributing, together with the surface roughness, to the decrease in the expected value. Moreover, the applied magnetic field may not have been sufficient to saturate the films. Liu *et al.* [5] studied an 80-Å film of magnetite on MgO/GaAs(100) by XMCD and obtained $m_s = 2.84\mu_B$/f.u. Orna *et al.* [1] investigated magnetite on MgO(100) over a wide thickness range and obtained $m_s = 1.83\mu_B$/f.u. for an 80-Å film and $m_s = 3.6\mu_B$/f.u. for a 580-Å film. Moussy *et al.* [3], using polarized neutron reflectometry (PNR), observed an increase in the total magnetic moment (m_{tot}) with thickness and found $m_{tot} = 3.2\mu_B$/f.u. for the thicker film (500 Å). The fact that a number of authors fail to obtain the bulk spin moment may be correlated with the difficulty of preparing well-ordered and stoichiometrically perfect films that are, moreover, free of additional iron oxide phases, e.g., wurtzite, maghemite, and hematite. Significant differences in XMCD results for bulk samples prepared by different methods have been reported, e.g., $3.90\mu_B$/f.u. for a cleaved crystal [14] and $1.70\mu_B$/f.u. for the same crystal which was polished [16]. This suggests that surface defects can generate great changes in the magnetic behavior, which is more noticeable in ultrathin films [2,9]. A summary of magnetic moments for Fe_3O_4 as determined by XMCD and other methods is given in Table I.

To our knowledge, there is no systematic study on magnetic spin moments with thicknesses in the range up to 50 Å. Regarding magnetization as a function of thickness there is some work on films starting from 80 Å, for example, an investigation by Orna *et al.* [1] between 80 and 3500 Å that correlates the magnetic behavior with the formation of antiphase boundaries at low thickness (t). They argued that since the antiphase boundary domain size (D) is larger (smaller) for thicker (thinner) films as $D \propto \sqrt{t}$, and magnetization depends

*gustavofmg@gmail.com

TABLE I. Magnetic moments (μ_B/f.u.) and coercive field (H_c) of Fe_3O_4 using XMCD,[a] VSM,[b] SQUID,[c] and polarized neutron reflectometry.[d]

Thickness	Substrate	m_s	m_{tot}	H_c (Oe)
25 Å [2]	$BaTiO_3$(100)	1.45[a]		140
26 Å (this work)	Ag(100)	2.7[a]	2.8[a]	300
26 Å (this work)	Pd(100)	3.2[a]	3.5[a]	
35 Å (this work)	Pd(100)	3.6[a]	4.0[a]	
50 Å [3]	α-Al_2O_3		2.4[d]	143
80 Å [1]	MgO(100)	1.83[a]		
80 Å [5]	MgO/GaAs(100)	2.84[a]	3.32[a]	
150 Å [3]	α-Al_2O_3		2.7[d]	383
580 Å [1]	MgO(100)	3.6[a]		
1000 Å [18]	MgO(001)	2.97[a]	4.08[b]	
1000 Å [18]	Al_2O_3(0001)	2.61[a]	3.6[b]	
Bulk [19]	Single crystal	3.68[a]	3.5[c]	
Bulk, polished [16]	Single crystal	1.70[a]		
Bulk, cleaved [14]	Single crystal	3.90[a]	4.2[a]	

on domain size [$M = M_S(1 - c/D)$, $c =$ constant, $M_S = 430.7$ emu/cm^3], this explains the decrease in magnetization with increasing thickness. For ultrathin magnetite films the obtained spin moments from several works present conflicting results. Reliable values for the spin moment are still missing and this work addresses this issue by experimentally determining m_s on Fe_3O_4 films of good surface quality with thicknesses near the unit-cell size. It is challenging to determine the thickness limit at which magnetite is formed and exhibits a bulk-like behavior.

We have performed a systematic investigation of the magnetic behavior of magnetite at room temperature by XMCD on a set of samples with thicknesses up to 45 Å. The *in situ* experiments were performed at the PGM beam line at the Laboratório Nacional de Luz Síncrotron (Campinas, Brazil), using an 80% circularly polarized light beam [17] ($P_c = 0.8$). We have prepared epitaxial, stoichiometric, and well-ordered magnetite ultrathin films in the [100] and [111] crystallographic directions and have followed the evolution of the spin and orbital magnetic moments, which were calculated using sum rules [15] of the integrated XMCD and total XAS spectra of Fe-$L_{2,3}$ edges. To our knowledge, we have for the first time observed the bulk spin magnetic moment for films thinner than 35 Å, and down to 10 Å we have still obtained significant spin moment values.

II. EXPERIMENTAL PROCEDURE

A series of ultrathin Fe_3O_4 samples with different thicknesses was prepared on single Pd(100) and Ag(100) crystals in ultrahigh vacuum ($p = 1 \times 10^{-10}$ mbar). Both crystals were prepared with cycles of 1-keV Ar-ion sputtering and subsequent annealing. Ultrathin films were grown on substrates by evaporating ultrahigh-purity Fe (e-beam source) in a controlled-O_2 environment. By varying the growth temperature, oxygen pressure, iron evaporation rate, and annealing after each growth, we have established a recipe to produce stoichiometric and well-ordered samples [20]. Ultrathin

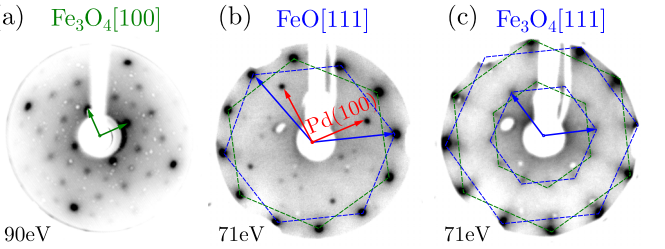

FIG. 1. (Color online) LEED patterns of (a) 16-ÅFe$_3$O$_4$[100] on Ag(100), (b) 7-ÅFeO[111] on Pd(100), and (c) 45-ÅFe$_3$O$_4$[111] on Pd(100).

Fe_3O_4(100) grows semiepitaxially on Ag(100) and, with proper annealing [20,21], exhibits excellent crystallographic order. We have used an iron evaporation rate of 0.6 Å/min (all growths) and an oxygen partial pressure of 2×10^{-7} mbar. The substrate was kept at 100°C during deposition, and after each growth the films were annealed at 450°C for 3 min at the same oxygen partial pressure used for growth. The absence of any kind of contamination was attested by the XAS spectra. The film thickness was determined by a previous calibration of the e-beam evaporator and was in good agreement with the thickness calculated by the integrated area of the Fe-L_3 edge.

Our samples exhibit good surface crystallographic order as attested by their low-energy electron diffraction (LEED) patterns, which were examined after each sample growth and soft annealing procedure. To illustrate this, in Fig. 1 we show the LEED patterns of three selected samples. Figure 1(a) is the diffraction pattern at 90 eV of a 16-Å-thick Fe_3O_4[100] grown on Ag(100), where the $(\sqrt{2} \times \sqrt{2})R45°$ surface reconstruction can be recognized [22]. Figures 1(b) and 1(c) show the [111] growth direction for two film thicknesses, both taken at the same energy (71 eV). As expected, FeO forms at lower coverage and we observe its diffraction pattern for the 7-Å-thick sample [Fig. 1(b)]. Moreover, the superimposed diffraction of the Pd(100) can also be seen at a lower intensity, which could indicate some island formation. The 45-Å-thick LEED pattern [Fig. 1(c)] indicates the formation of Fe_3O_4[111], consisting of four domains rotated by 90° with respect to each other, as already observed for Fe_3O_4(111)/Pt(100) [23]. Although we used a different substrate, this is quite reasonable, since Pd and Pt have the same fcc structure and almost the same lattice parameters, 3.89 and 3.92 Å, respectively.

The left sides of Figs. 2(a) and 2(b) show the evolution of XAS spectra at the Fe-$L_{2,3}$ edge with increasing film thickness for the [100] and [111] growth directions, respectively. All spectra are shown on the same intensity scale as for the thicker film (45 Å). For both growth directions the energy positions of the Fe-L_2 and Fe-L_3 peaks and the observed shoulders (see arrows in figures) that appear in absorption spectra at higher coverages are typical of magnetite [2]. Furthermore, our ultrathin films exhibit dichroic peaks with the expected intensities for stoichiometric magnetite.

The three most common methods of measuring soft x-ray absorption spectra are transmission mode, fluorescence yield, and total electron yield (TEY). We have used TEY, which is the most surface-sensitive mode, with a probing depth of about 20–30 Å. For XMCD experiments a magnetic field of 9 kOe

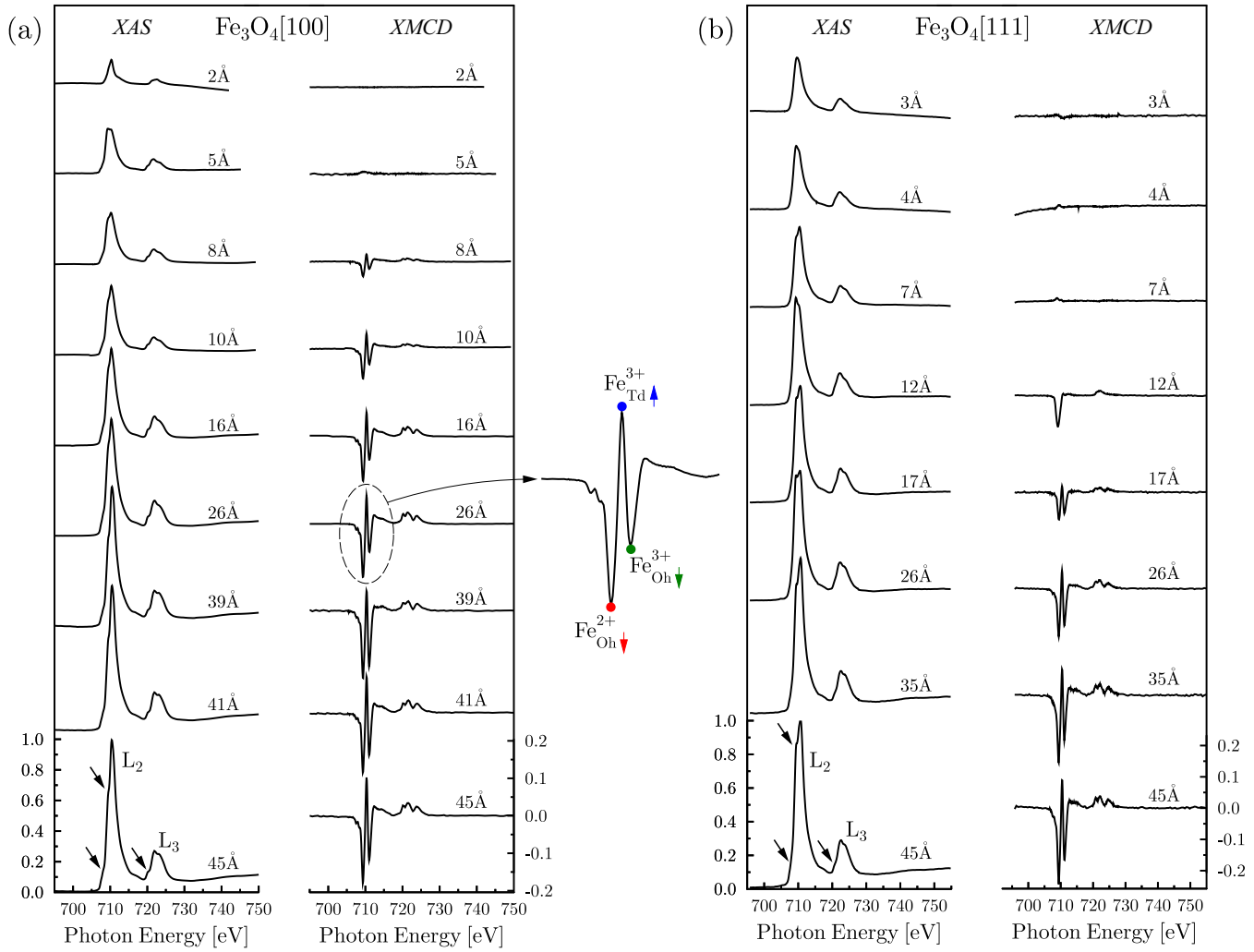

FIG. 2. (Color online) (a) XAS and XMCD of Fe_3O_4[100] at the Fe-$L_{2,3}$ edge; (b) XAS and XMCD of Fe_3O_4[111]. XAS and XMCD spectra are all shown on the same intensity scale as for the 45-Å-thick samples.

was applied parallel to the light beam and at 60° with respect to the film plane. We have performed magnetic optical Kerr effect (MOKE) measurements and we could not saturate the film in polar geometry and, with a relative low magnetic field, saturate in the film plane (longitudinal MOKE). So we concluded that our films have an in-plane easy axis, and magnetization is in-plane also for XMCD measurements.

A. Fe_3O_4[100]

The absorption spectra of Fe_3O_4[100] [Fig. 2(a)] show an increase in the XAS signal with thickness and the intensity is almost saturated at 45 Å. From intensity × coverage we have calculated a mean free path of 15 ± 3 Å, which is in agreement with Ref. [14] and confirms our previous thickness calibration.

The XMCD spectra of Fe_3O_4[100] are shown at the right in Fig. 2(a). For the 2- and 5-Å-thick samples no dichroic signal is observed, an indication that magnetite has not yet been formed. LEED and scanning tunneling microscopy studies of iron oxide grown on Pt(100) [23] and Pt(111) [24,25] have shown that, up to two monolayers, the film grows as FeO(111) (paramagnetic), and at higher coverage it changes to Fe_3O_4(111). For these thinner films FeO islands are probably formed, as observed by low-energy electron microscopy [9] and by scanning tunneling microscopy [24,25]. The thickness to complete a full unit cell in the [100] direction is 8.4 Å (the lattice parameter of Fe_3O_4), and coincidentally, the first typical dichroic signal for magnetite [14,19] that we observe is for an 8-Å-thick sample. Above that, the dichroic signal increases with thickness, as well as the XAS intensity. Films thicker than 26 Å exhibit typical signatures of stoichiometric magnetite.

B. Fe_3O_4[111]

Figure 2(b) shows the XAS and XMCD spectra for Fe_3O_4[111] on Pd(100) prepared as already described. The dependence of the XAS signal on the thickness is quite similar to that in the [100] direction, and a mean free path of 11 ± 3 Å has been calculated.

No dichroic signal is observed for samples with thicknesses of less than 7 Å, which are most probably FeO. The thickness to complete a full unit cell in the [111] direction is 14.6 Å. The question that arises here is what structure (and magnetic

properties) assumes a film with a thickness close to that needed to complete a full unit cell. The first dichroic signal is observed for the 12-Å-thick film, which does not exhibit Fe^{3+}dichroic peaks but shows a pronounced negative peak at the position for Fe^{2+} ions located at the octahedral site. We consider the possibility that magnetite is close to being formed, but due to the incomplete unit cell, the Fe^{3+} ions cannot be precisely assigned to octahedral and tetrahedral sites and may cancel each other. A detailed structural investigation at this thickness would be necessary to clarify this point, but that is beyond the present investigation.

As shown in Fig. 2(b), only above 17 Å do we have a typical XMCD spectrum of bulk magnetite. Again, as for the [100] direction the dichroic signal increases with the thickness and almost saturates at 45 Å.

C. Ferrimagnetic hysteresis of Fe_3O_4

Bulk Fe_3O_4 has an inverse spinel structure, with the Fe^{2+} cations occupying the octahedral sites and the Fe^{3+} ions occupying the octahedral (O_h) and tetrahedral (T_d) sites. The formula is written as $[Fe^{3+}_{\uparrow}]_{T_d}[Fe^{2+}_{\downarrow}Fe^{3+}_{\downarrow}]_{O_h}O_4$, with the spins coupled ferromagnetically at the O_h site and antiferromagnetically at the T_d site. The spin magnetic moment contributions from $Fe^{3+}_{T_d}$ ($-5\mu_B$) and $Fe^{3+}_{O_h}$ ($+5\mu_B$) cancel each other, and the net spin moment is theoretically due only to $Fe^{2+}_{O_h}$ ($+4\mu_B$).

Monitoring the XMCD intensity of the L_3 edge peaks related to $Fe^{2+}_{O_h}$, $Fe^{3+}_{T_d}$, and $Fe^{3+}_{O_h}$, we have extracted the hysteresis loops by calculating

$$I_{\mathrm{XMCD}}(H) = \left(T^{\mathrm{RCP}}_{\mathrm{Fe}}\right)/\left(T^{\mathrm{RCP}}_{\mathrm{Bkg}}\right) - \left(T^{\mathrm{LCP}}_{\mathrm{Fe}}\right)/\left(T^{\mathrm{LCP}}_{\mathrm{Bkg}}\right),$$

where T^{RCP} and T^{LCP} are the TEY intensities as a function of the applied field (-4.5 kOe $\rightarrow$ 4.5 kOe) for right and left circularly polarized light, respectively. T_{Fe} denotes the intensity of each iron ion peak ($Fe^{2+}_{O_h}$, $Fe^{3+}_{T_d}$, $Fe^{3+}_{O_h}$), and T_{Bkg} the background intensity at 700 eV, which is used to normalize the intensities. Figure 3(a) shows the hysteresis loops for the 26-Å-thick Fe_3O_4[100] sample for each of the ion peaks of the XMCD Fe-L_2 edge. All three hysteresis loops exhibit a typical ferromagnetic behavior, almost saturated and with a coercive field of 300 Oe, close to reported values [2,3,6,10,11,13]. The hysteresis of $Fe^{3+}_{T_d}$ has the opposite magnetization direction compared to $Fe^{2+}_{O_h}$ and $Fe^{3+}_{O_h}$.

When we naively sum the three iron ions' contributions, $I(Fe^{3+}_{T_d}) + I(Fe^{3+}_{O_h}) + I(Fe^{2+}_{O_h})$, as shown in Fig. 3(b), the total hysteresis should exhibit the macroscopic ferrimagnetic response as measured by techniques such as MOKE, vibrating sample magnetometry (VSM), and superconducting quantum interference device (SQUID). As XMCD (measured in the TEY mode) is both a surface-sensitive and an element-specific method, we probably obtained only the ferrimagnetic response from the 26-Å-thick magnetite film, without any other contributions. It should be mentioned that in order to correctly extract the magnetic moment from XMCD measurements, not only should the peak maxima be used, but also the entire dichroic signal must be considered, using sum rules. This is done in the next subsection.

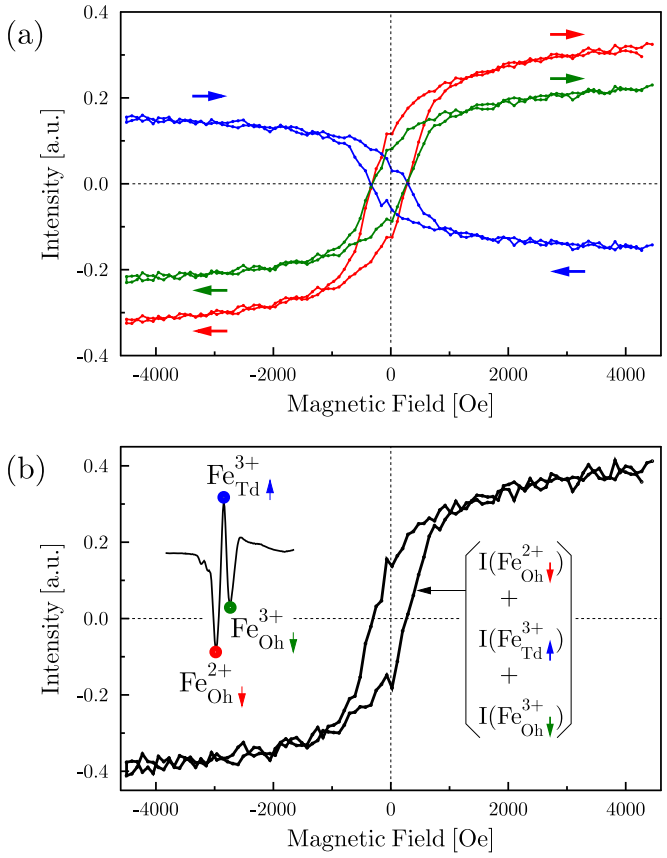

FIG. 3. (Color online) (a) Hysteresis loops from the intensity of $Fe^{2+}_{O_h}$ (red), $Fe^{3+}_{T_d}$ (blue), and $Fe^{3+}_{O_h}$ (green) peaks. (b) Hysteresis loop from the sum of the three ions' contributions to the XMCD signal at the Fe-L_2 edge.

D. Magnetic moments

For Fe_3O_4[100] above 8 Å and for Fe_3O_4[111] above 12 Å we have calculated the spin and orbital magnetic moments by applying sum rules. We have considered XMCD signals from 695 to 750 eV and assumed the number of holes in the 3*d* band to equal 13.5 as in Ref. [14]. As the angle between the magnetization and the x-ray propagation direction is 60°, XMCD spectra were normalized by $P_c\cos(60^\circ)$.

The evolutions of the spin magnetic moment for magnetite [100] and [111] are quite similar for both directions as shown in Fig. 4. Ten-angstrom-thick magnetite films already present significant magnetic moments. The spin moment value for the 17-Å sample is higher than that reported for thicker films [1,2]. The magnetic moment of our 26-Å-thick film is twice the value for a 25-Å film [2], comparable to those reported for 80 Å [5] and 150 Å [3] and even higher than the value for a 1000-Å film [19] (see Table I).

The spin moment increases with the thickness and saturates at approximately 35 Å. The observed saturation value is $3.6\mu_B$/f.u. for the [111] orientation, which is in agreement with the values obtained for thicker magnetite films (580–1000 Å) [1,18,19]. A ^{57}Fe-Mössbauer study of ultrathin (18- to 50-Å) Fe_3O_4 [8] has shown a breakdown of the long-range ferromagnetic order below 35 Å, in line with our observations. Moreover, they found a fully paramagnetic state at 18 Å. We

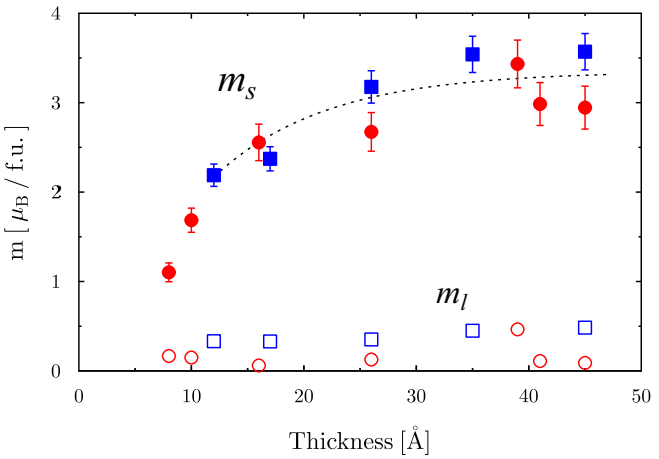

FIG. 4. (Color online) Spin moment m_S (filled symbols) and angular moment m_l (open symbols) of [100]-magnetite (circles) and [111]-magnetite (squares) as a function of the thickness. The dashed line is a guide for the eyes.

could observe a magnetite dichroic signature above 17 Å for Fe_3O_4[111] and above 8 Å for Fe_3O_4[100].

Several authors that have used the TEY mode in XMCD of Fe_3O_4 above 30 Å (and thicker) have found spin magnetic moments below the bulk value; see Table I. This is probably related to the fact that the probe depth of the TEY mode is around 20 Å and, therefore, quite sensitive to the surface quality. Defective sample surfaces would cause a decrease in the spin moment, as observed, e.g., for a polished sample [16]. When the magnetic moment is measured by techniques that probe the entire sample (e.g., SQUID and VSM) and the surface-to-volume ratio is low, surface defects can be neglected. Wong *et al.* [13] have measured a 50-Å-thick magnetite film by SQUID and obtained bulk saturation magnetization. Our samples have good surface crystallographic order as attested by LEED and exhibit stoichiometric magnetite dichroic signals. Those features are essential for obtaining the spin magnetic moment of true (bulk-like) magnetite in the ultrathin limit. Ultrathin samples obtained by other authors [1,2,5,9] in general exhibit XMCD intensities that suggest either off-stoichiometry or the presence of mixed phases.

Because of superparamagnetic behavior, our thinner films (<26 Å) may require higher magnetic fields to saturate completely. This could be why they did not present the bulk spin moment. Using higher fields or cooling the sample could solve this issue. Moreover, ultrathin films may present other contributions to moment lowering, such as magnetic surface effects, defects, roughness, and mixed phases.

We are aware of the saturation effects intrinsic to the TEY detection mode. As a matter of fact, their correction could lead to slightly higher values for the spin moments but decrease the orbital values, which could take our result even closer to the bulk ones [14]. Furthermore, as pointed out in Ref. [14], the XMCD signal of magnetite samples can extend well beyond the Fe-L_2 edge. In our case, given the limited amount of beam time available, we chose to use shorter scans for several values of thickness. This choice can also lead to underestimated values of the spin moment and overestimated values of the orbital moment [14]. In any case, neither of these effects would compromise the conclusion obtained in this work, given that here we are interested in the trends of these measurements with the thickness, which by no means depend on detailed application of the XMCD sum rules.

III. CONCLUSIONS

In summary, we have followed the evolution of the magnetic moment of ultrathin Fe_3O_4 as a function of the thickness (8–45 Å). The stoichiometry and surface quality of the films have been attested by XAS, XMCD, and LEED. At low thicknesses FeO has probably been formed and evolved to Fe_3O_4 above the thickness of 1 unit cell. We have observed for the first time an atypical dichroic spectrum for a 12-Å-thick film [see Fig. 2(b)], which may indicate an intermediate structure between FeO and Fe_3O_4 and, for this sample, a novel magnetic state. For both the [100] and the [111] orientations we observe a characteristic dichroic signature of magnetite around the unit-cell thickness, however, with a lower spin moment that evolves to the bulk value for thicker films. The hysteresis curves for each iron ion site have been measured by XMCD for a 26-Å-thick [100]-magnetite sample, exhibiting ferrimagnetic behavior and a coercive field of 300 Oe. A spin moment of $3.6\mu_B$/f.u. was found at 35 Å for Fe_3O_4 [111]. These results are direct evidence that both the ferrimagnetic order and the bulk moment value are preserved at room temperature around the thickness of 2 unit cells. We have also shown that even 10-Å-thick magnetite already presents a significant magnetic moment. We believe that the conclusions of this work are of great importance, especially if magnetite layers down to subnanoscale thickness are employed in spin electronics devices.

ACKNOWLEDGMENTS

The authors thank CNPq, FAPEMIG, FAPESP, and CAPES, Brazilian research agencies, for financial support and the Laboratório Nacional de Luz Síncrotron for beam time (SGM-10986 and SGM-12716).

[1] J. Orna, P. A. Algarabel, L. Morellón, J. A. Pardo, J. M. de Teresa, R. López Antón, F. Bartolomé, L. M. García, J. Bartolomé, J. C. Cezar, and A. Wildes, Phys. Rev. B **81**, 144420 (2010).

[2] V. Hari Babu, R. K. Govind, K.-M. Schindler, M. Welke, and R. Denecke, J. Appl. Phys. **114**, 113901 (2013).

[3] J.-B. Moussy, S. Gota, A. Bataille, M.-J. Guittet, M. Gautier-Soyer, F. Delille, B. Dieny, F. Ott, T. D. Doan, P. Warin, P. Bayle-Guillemaud, C. Gatel, and E. Snoeck, Phys. Rev. B **70**, 174448 (2004).

[4] P. Morrall, F. Schedin, S. Langridge, J. Bland, M. F. Thomas, and G. Thornton, J. Appl. Phys. **93**, 7960 (2003).

[5] W. Q. Liu, Y. B. Xu, P. K. J. Wong, N. J. Maltby, S. P. Li, X. F. Wang, J. Du, B. You, J. Wu, P. Bencok, and R. Zhang, Appl. Phys. Lett. **104**, 142407 (2014).

[6] Y. X. Lu, J. S. Claydon, Y. B. Xu, D. M. Schofield, and S. M. Thompson, J. Appl. Phys. **95**, 7228 (2004).
[7] W. Eerenstein, T. Hibma, and S. Celotto, Phys. Rev. B **70**, 184404 (2004).
[8] F. C. Voogt, T. T. M. Palstra, L. Niesen, O. C. Rogojanu, M. A. James, and T. Hibma, Phys. Rev. B **57**, R8107 (1998).
[9] M. Monti, B. Santos, A. Mascaraque, O. Rodríguez de la Fuente, M. A. Niño, T. O. Mentes, A. Locatelli, K. F. McCarty, J. F. Marco, and J. de la Figuera, Phys. Rev. B **85**, 020404 (2012).
[10] Y. X. Lu, J. S. Claydon, Y. B. Xu, S. M. Thompson, K. Wilson, and G. van der Laan, Phys. Rev. B **70**, 233304 (2004).
[11] Y. X. Lu, J. S. Claydon, E. Ahmad, Y. B. Xu, M. Ali, B. J. Hickey, S. M. Thompson, J. A. D. Matthew, and K. Wilson, J. Appl. Phys. **97**, 10C313 (2005).
[12] F. Schedin, L. Hewitt, P. Morrall, V. N. Petrov, G. Thornton, S. Case, M. F. Thomas, and V. M. Uzdin, Phys. Rev. B **58**, R11861 (1998).
[13] P. K. J. Wong, W. Zhang, X. G. Cui, Y. B. Xu, J. Wu, Z. K. Tao, X. Li, Z. L. Xie, R. Zhang, and G. van der Laan, Phys. Rev. B **81**, 035419 (2010).
[14] E. Goering, S. Gold, M. Lafkioti, and G. Schütz, Europhys. Lett. **73**, 97 (2006).
[15] C. T. Chen, Y. U. Idzerda, H.-J. Lin, N. V. Smith, G. Meigs, E. Chaban, G. H. Ho, E. Pellegrin, and F. Sette, Phys. Rev. Lett. **75**, 152 (1995).
[16] E. J. Goering, M. Lafkioti, S. Gold, and G. Schuetz, J. Magn. Magn. Mater. **310**, e249 (2007).
[17] J. J. S. Figueiredo, R. Basilio, R. Landers, F. Garcia, and A. de Siervo, J. Synch. Rad. **16**, 346 (2009).
[18] M. Kallmayer, K. Hild, H. J. Elmers, S. K. Arora, H.-C. Wu, R. G. S. Sofin, and I. V. Shvets, J. Appl. Phys. **103**, 07D715 (2008).
[19] D. J. Huang, C. F. Chang, H.-T. Jeng, G. Y. Guo, H.-J. Lin, W. B. Wu, H. C. Ku, A. Fujimori, Y. Takahashi, and C. T. Chen, Phys. Rev. Lett. **93**, 077204 (2004).
[20] G. J. P. Abreu, R. Paniago, and H.-D. Pfannes, J. Magn. Magn. Mater. **349**, 235 (2014).
[21] D. Bruns, S. R. Lindemann, K. Kuepper, T. Schemme, and J. Wollschläger, Appl. Phys. Lett. **103**, 052401 (2013).
[22] M. Fonin, R. Pentcheva, Y. S. Dedkov, M. Sperlich, D. V. Vyalikh, M. Scheffler, U. Rüdiger, and G. Güntherodt, Phys. Rev. B **72**, 104436 (2005).
[23] M. Ritter, H. Over, and W. Weiss, Surf. Sci. **371**, 245 (1997).
[24] M. Ritter, W. Ranke, and W. Weiss, Phys. Rev. B **57**, 7240 (1998).
[25] W. Weiss and M. Ritter, Phys. Rev. B **59**, 5201 (1999).